Stem Cell Reports
Article
OPEN ACCESS

Preferential Propagation of Competent SIX2+ Nephronic Progenitors by LIF/ROCKi Treatment of the Metanephric Mesenchyme

Shunsuke Tanigawa,[1,2,3] Nirmala Sharma,[1] Michael D. Hall,[1] Ryuichi Nishinakamura,[2,3] and Alan O. Perantoni[1,*]
[1]National Cancer Institute-Frederick, Frederick, MD 21702, USA
[2]Department of Kidney Development, Institute of Molecular Embryology and Genetics
[3]Program for Leading Graduate Schools, Health Life Science: Interdisciplinary and Glocal (Global and Local) Oriented Program
Kumamoto University, 2-2-1 Honjo, Kumamoto 860-0811, Japan
*Correspondence: perantoa@mail.nih.gov
http://dx.doi.org/10.1016/j.stemcr.2015.07.015

SUMMARY

Understanding the mechanisms responsible for nephrogenic stem cell preservation and commitment is fundamental to harnessing the potential of the metanephric mesenchyme (MM) for nephron regeneration. Accordingly, we established a culture model that preferentially expands the MM SIX2+ progenitor pool using leukemia inhibitory factor (LIF), a Rho kinase inhibitor (ROCKi), and extracellular matrix. Passaged MM cells express the key stem cell regulators *Six2* and *Pax2* and remain competent to respond to WNT4 induction and form mature tubular epithelia and glomeruli. Mechanistically, LIF activates STAT, which binds to a *Stat* consensus sequence in the *Six2* proximal promoter and sustains SIX2 levels. ROCKi, on the other hand, attenuates the LIF-induced differentiation activity of JNK. Concomitantly, the combination of LIF/ROCKi upregulates *Slug* expression and activates YAP, which maintains SIX2, PAX2, and SALL1. Using this novel model, our study underscores the pivotal roles of SIX2 and YAP in MM stem cell stability.

INTRODUCTION

Although considerable progress has been made in understanding the cues that direct self-renewal and differentiation of pluripotent stem cells (Buehr et al., 2008), the factors and pathways capable of perpetuating any multipotent tissue-specific progenitor in the absence of immortalizing genetic modifications remain largely undefined. During development, reciprocal interactions between the ureteric bud (UB) and the surrounding metanephric mesenchyme (MM) direct the formation of the metanephros. The MM promotes the branching morphogenesis of the UB to generate the collecting duct network. In turn, the UB induces condensation and mesenchymal-epithelial transition (MET) in the MM to initiate nephron formation at each bud tip. Condensed cells of the MM cap the tips of the branching UB in the cortical nephrogenic zone of the metanephros and provide a self-renewing population of SIX2+ progenitors, which supply the precursors for nephronic epithelia (Kobayashi et al., 2008). Ablation of *Six2* results in the premature commitment of these progenitors and a depletion of the progenitor pool. Therefore, SIX2 is a major determinant in the maintenance and self-renewal of the nephronic precursor. The aggregate SIX2-expressing population is further regulated by the transcriptional co-activator and Hippo pathway component Yes-associated protein (YAP) and is growth-limited by signals emanating from the encapsulating cortical stroma (Das et al., 2013). The loss of stromal signals promotes the expansion of undifferentiated SIX2+ stem cells, stimulates the nuclear localization of YAP, and inhibits the formation of nephronic structures. Conversely, *Yap* ablation causes renal hypoplasia, characterized by a measureable deficit in progenitor self-renewal and fewer nephrons. These findings led us to hypothesize that constitutive activation of SIX2 and YAP is sufficient to sustain this tissue-specific stem cell.

During development, extrinsic signals in a progenitor's microenvironment provide cues for self-renewal and lineage commitment. Although several growth factors, including fibroblast growth factors (FGFs) 2 (Perantoni et al., 1995), 8 (Perantoni et al., 2005), 9, and 20 (Barak et al., 2012) and epidermal growth factor (EGF)/transforming growth factor α (TGF-α) (Rogers et al., 1992), support the survival of MM cells and facilitate the limited expansion of this population in culture, they have proven to be insufficient for long-term propagation of progenitors with stem-like properties and nephronic potential. In this study, we optimize the niche for rat progenitors using growth factors, extracellular matrix, and Rho kinase inhibitor, which, in combination, sustain SIX2 and YAP nuclear expression. Moreover, we demonstrate that these factors contribute to the preferential propagation and partial stabilization of MM progenitors with the preservation of stem cell markers and a capacity for differentiation.

RESULTS

The Extracellular Matrix Helps Stabilize MM Progenitors

Primary cultures of MM were generated from developmentally comparable embryonic day (E) 13.5 rat or E11.5 mouse

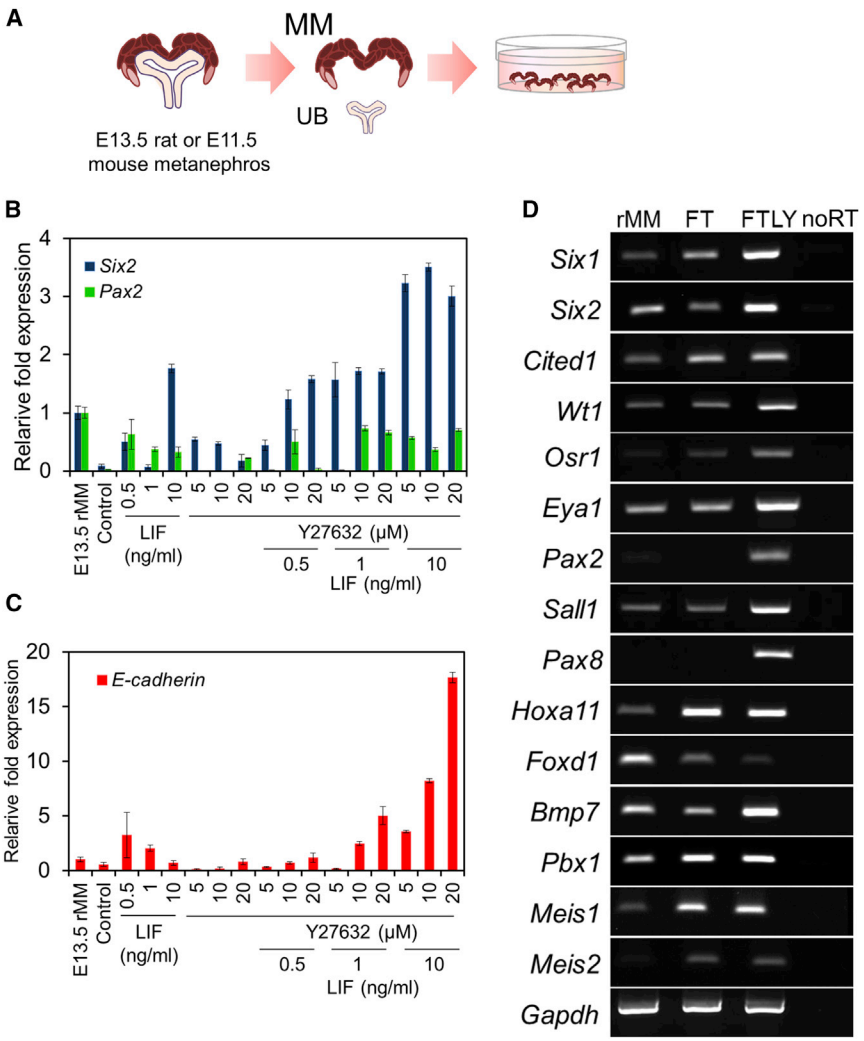

Figure 1. LIF and Y27632 Support the Retention of Progenitor Marker Expression in Cultured MMs

(A) Schematic of the MM cell culture method. Isolated rat or mouse MMs were explanted on culture dishes in serum-free medium.

(B and C) Expression levels of the progenitor markers *Six2* and *Pax2* (B) and the differentiation marker *E-cadherin* (C) in cells grown in control (FT) medium or LIF or Y27632 for 10 days on laminin. Uncultured rMMs at E13.5 were used for comparison.

(D) RT-PCR expression profiles for cells grown in FT or FTLY medium on fibronectin. Uncultured rMMs served as controls. noRT, no reverse transcriptase control.

metanephric rudiments (Figure 1A). MMs were dissected from trypsin-treated metanephroi and cultured as intact masses (10/60-mm dish) for up to 10 days using 50 ng/ml FGF2 and 10 ng/ml TGF-α (referred to as FT medium) to promote the survival and growth of cells (Perantoni et al., 1995; Plisov et al., 2001). To establish whether these conditions support progenitor self-renewal, primary cultures of rat MMs (rMMs) in FT medium were analyzed for markers associated with cap mesenchyme or MM progenitor maintenance, i.e., *Six2*, *Pax2* (Kobayashi et al., 2008; Torres et al., 1995), and *Cited1* (Plisov et al., 2005), by qPCR (Figure 1B; Figure S1A). Compared with uncultured rMM controls, cells grown on regular tissue culture dishes showed substantial loss of expression of each of these markers, indicating that FT conditions were inadequate for long-term SIX2+ progenitor propagation. To stabilize stem cell marker expression, culture conditions were modified through the addition of matrix coatings, growth factors, and small-molecule inhibitors.

The extracellular matrix associated with nephron formation is restructured radically at MET in vivo. During this morphogenesis, laminin replaces fibronectin in newly formed epithelia (Ekblom et al., 1980). To determine whether the matrix itself helps stabilize the progenitors, primary explants (2/well) in FT medium were seeded onto matrix-coated, 24-well culture dishes and examined after 10 days for expression of progenitor markers and cell proliferation. Compared with dishes bearing no matrix, cells on fibronectin or laminin expressed elevated levels of the progenitor markers *Six2* and *Cited1* (Figure S1A). Matrigel stimulated a 10-fold increase in the epithelial marker *Lim1*, suggesting that cells were differentiating on this coating, and its use was discontinued. Cell proliferation was also evaluated, but cell numbers were not significantly affected by changes in matrix (Figure S1B). Given the ability of matrix coatings to elevate the expression of stem markers, fibronectin- or laminin-coated dishes were employed in all subsequent studies.

LIF and the Rho Kinase Inhibitor Y27632 Support the Self-Renewal of MM Progenitors

Leukemia inhibitory factor (LIF) induces MET in primary rMM cells, generating tubules and glomerulus-like structures (Barasch et al., 1999; Plisov et al., 2001). It is expressed both by the UB and MM, whereas LIF receptors are found

on cap progenitors and newly formed nephronic epithelia (Plisov et al., 2001). Because LIF treatment also greatly expanded the size of rMM explants, we postulated a role for LIF in rMM self-renewal. Moreover, the Rho kinase inhibitor Y27632 or a dominant-negative *RhoA* construct also increased the size of cultured mouse MM (mMM) colonies (Osafune et al., 2006). Accordingly, we investigated the ability of these two factors to regulate the growth of rMMs in culture. For this, ten primary rMM explants were seeded onto fibronectin-coated wells of 6-well dishes and treated for 10 days, with medium replacement every 2–3 days. Individually both LIF (1 ng/ml) and Y27632 (10 μM) nearly doubled cell counts relative to controls in FT medium, and simultaneous treatment yielded numbers nearly four times those of controls, demonstrating that both factors contribute independently to the proliferation of rMMs (Figure S1C). Furthermore, 5 ng/ml LIF yielded no significant increase over the 1 ng/ml treatment, suggesting that the lower level is optimal for growth. Based on final cell counts, the population expansion was achieved with more than eight cell doublings during the 10-day period.

To determine whether LIF stimulation or Rho kinase inhibition stabilized the expression of stem cell markers, cells were evaluated for *Six2* and *Pax2* expression. Cultured rMMs were treated with LIF (0.5–10 ng/ml) or Y27632 (5.0–20 μM) in FT medium to maximize marker expression and minimize any concomitant stimulation of expression of the differentiation marker *E-cadherin*. For these studies, primary explants of MM (3/well in a 24-well laminin-coated plate) were cultured for 10 days and then analyzed by qPCR. Overall, the highest concentrations of LIF and Y27632 supported the most robust expression of *Six2* and *Pax2* (Figure 1B). Levels of *Six2* expression were three times greater than those observed in uncultured rMMs, whereas *Pax2* levels approached those of uncultured MMs. However, *E-cadherin* expression was also elevated greatly (>15-fold), suggesting that these higher levels shifted the balance between stemness and commitment to MET (Figure 1C). In combination with FT factors, lower levels of LIF (1 ng/ml) and Y27632 (10 μM) provided the best balance, supporting expression of both stem cell markers with only a 2-fold induction of *E-cadherin*. This will be referred to hereafter as FTLY medium. When the study was expanded to evaluate the expression of several markers of intermediate mesoderm, rMMs, condensed mesenchyme (e.g., *Cited1*, *Pax2/8*, *Osr1*, *Sall1*, *Six1/2*, and *Wt1*), or stroma (*Foxd1*, *Pbx1*, and *Meis1/2*) by semiquantitative RT-PCR, the expression levels of FTLY-treated cells were generally equal to or greater than those of the progenitors (rMM lane) from which they were derived (Figure 1D). Again, FT-treated cultures failed to maintain *Pax2* expression. *Bmp7* has previously been linked to proliferation of these progenitors (Blank et al., 2009), and our conditions also stabilized its expression, suggesting that stimulation of growth may be mediated in part by this factor. Interestingly, the stromal progenitor marker *Foxd1* was greatly reduced in FTLY medium, whereas the stromal markers *Pbx1* and *Meis 1/2* increased, suggesting that FTLY either does not support self-renewal of stromal progenitors or that it facilitates their conversion to SIX2+ progenitors, which is less likely given the increased *Pbx1/Meis1/2* levels with FT and FTLY media.

Progenitor status was further documented by immunofluorescence (IF) staining for the stem cell markers SIX2, PAX2, and SALL1, all of which localize to the nucleus during development (Figure 2A; Figure S2). Cells were grown for 10 days in FTLY medium and then dissociated and replated in FT or FTLY medium for 3 additional days on laminin-coated, 4-well chamber slides (50,000 cells/well). When probed for SIX2, rMM cells showed frequent nuclear staining in FTLY-treated cultures but only limited staining in FT-treated control cultures. Similarly, nuclear staining for PAX2 was more prominent in FTLY-treated cultures. SALL1, on the other hand, was detected in the nuclei of both control (FT-treated) and FTLY-treated cultures (Figure S2). These observations are consistent with our results from gene expression studies and suggest an association between FTLY treatment and the increased incidence of SIX2 nuclear expression.

To quantify the effects of FTLY treatment on the SIX2+ progenitor population in mixed MM cultures, cells were analyzed for nuclear expression of SIX2 or the stromal marker PBX1 (Boivin et al., 2015) by IF. Freshly isolated rMMs contained ~30% SIX2+ and 70% PBX1+ cells (Figures 2B and 2C). For unpassaged cells, 3 explants/well were dispersed by pipetting and seeded in 4-well, fibronectin-coated chamber slides. With FTLY treatment for 7 days, the SIX2+ population increased to nearly 50%, whereas FT treatment caused a 50% decline in the SIX2+ population. Therefore, FTLY not only sustained the SIX2+ progenitors but also preferentially expanded this population. To assess the population dynamics in subsequent passages, cells were dissociated with trypsin and evaluated as monolayer cultures. Confluent cells were trypsinized and seeded into chamber-slide wells (50,000 cells/well) with fixation the following day. The SIX2+ population peaked at over 65% by passage 2. By passage 3, however, the FTLY-expanded SIX2+ population declined and was largely replaced by SIX2−/PBX1−/CADHERIN6(CDH6)+ epithelium-like clusters (Figure S3). CDH6 is primarily expressed in newly formed nephronic epithelium (Cho et al., 1998), suggesting that the SIX2+ cells had initiated MET. These clusters did not stain for E-CADHERIN (ECDH, data not shown), consistent with progression only to primitive epithelium. Regardless, a significant percentage of cells (~8%) remained SIX2+ in FTLY-treated

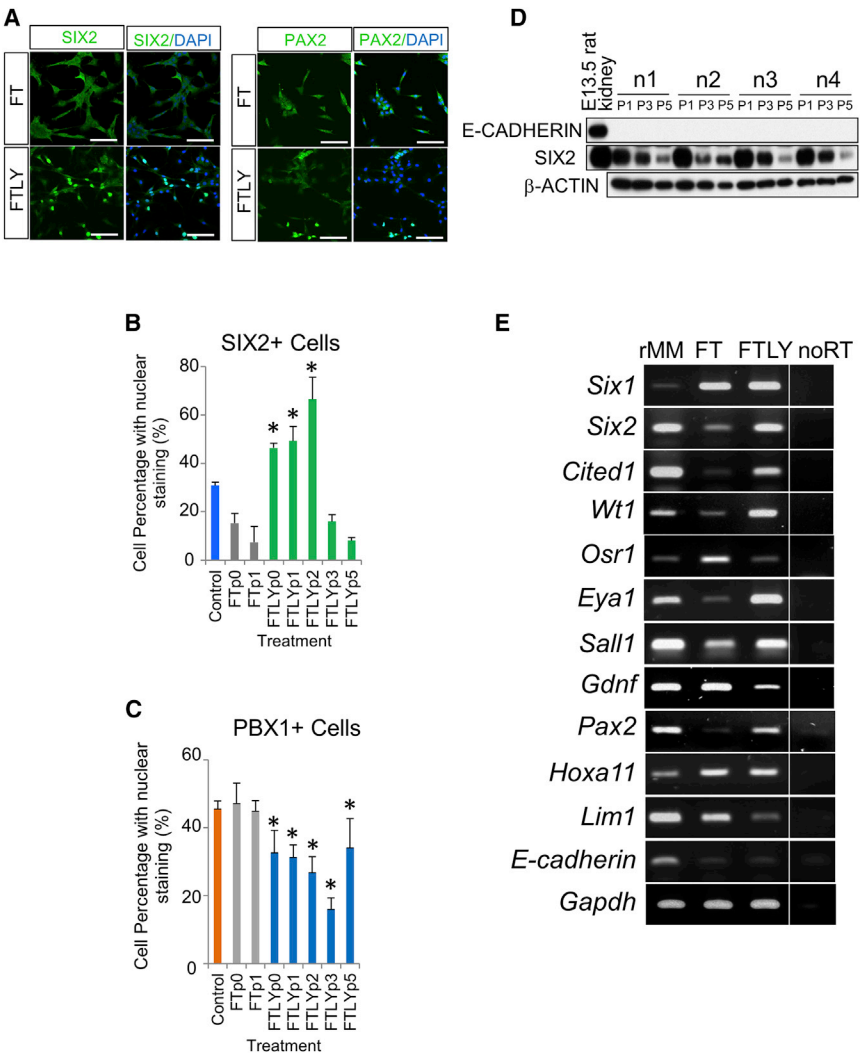

Figure 2. FTLY Preferentially Expands the SIX2+ MM Progenitor

(A) FTLY medium preserves nuclear staining for SIX2 and PAX2. Scale bars, 100 μm.

(B) FTLY medium significantly increases the proportion of SIX2+ progenitors over time/passaging in mixed rMM populations (*$p < 0.05$). Error bars show variation from three to four independent cultures.

(C) FTLY treatment significantly decreases the proportion of PBX1+ stromal cells over time/passaging. (*$p < 0.05$). Error bars show variation from three to four independent cultures.

(D) SIX2 expression levels decline with rMM passaging (P) in four separate cultures (n1–n4). E-CADHERIN is not detected.

(E) FTLY treatment preserves the expression of progenitor markers despite multiple (five) passages. Uncultured rMMs served as controls.

passage 5 cultures, demonstrating that SIX2+ progenitors are preserved and persist in multi-passaged populations. Immunoblots also showed a decline in SIX2 protein levels from four separate cultures of rMM cells at passages 1, 3, and 5 (Figure 2D), consistent with the loss of SIX2+ cells. Concordant with immunostaining, ECDH was not detected in later passages.

We further examined the ability of FTLY medium to sustain the expression of several progenitor markers in long-term cultures. RT-PCR gene expression profiles were generated from passage 5 cells. For this, cells were briefly trypsinized (2–3 min) and split one to three. Cells were then passaged just prior to reaching confluence (every 4–5 days). Therefore, by passage 5, cells had been in culture for nearly 1 month. The profile for passage 5 FTLY-treated MMs still closely resembled that for uncultured rMMs with retention of *Six2*, *Eya1*, *Sall1*, *Cited1*, *Pax2*, and *Hoxa11*, whereas the differentiation markers *Lim1* and *E-cadherin* were reduced greatly (Figure 2E). On the other hand, FT-treated cultures showed reduced levels of expression of most of the progenitor markers relative to FTLY treatment, demonstrating a significant improvement in long-term progenitor maintenance.

LIF/Rho Kinase Inhibitor Preserves the Capacity of rMM Progenitors to Respond to Inductive Signaling

To assess whether progenitors retained an ability to epithelialize upon cue, rMMs grown in FT or FTLY medium for 10 days were trypsinized and plated in FT medium without or with WNT4 (100 ng/ml). Expression of the differentiation markers *Lim1* and *E-cadherin* was upregulated 3- to 4-fold with a 72-hr WNT4 treatment (Figure 3A). Passage 5 cells also responded to a 3-day induction with LIF (50 ng/ml) or the GSK3β inhibitor CHIR99021 (1 μM) by upregulating the expression of the differentiation markers *Lim1* and *E-cadherin* only when cells had been propagated continuously in FTLY medium (Figure 3B). To evaluate this responsiveness more rigorously, primary and passaged rMM cells were assessed for their ability to form colonies on WNT4-expressing NIH 3T3 cells. Only multipotent MM progenitors generate colonies in this assay and exhibit multi-lineage differentiation from a single progenitor (Osafune et al., 2006). For these studies, WNT4-expressing NIH 3T3 cells that had been placed in stasis by treatment with mitomycin C were seeded into wells (500,000 cells/well)

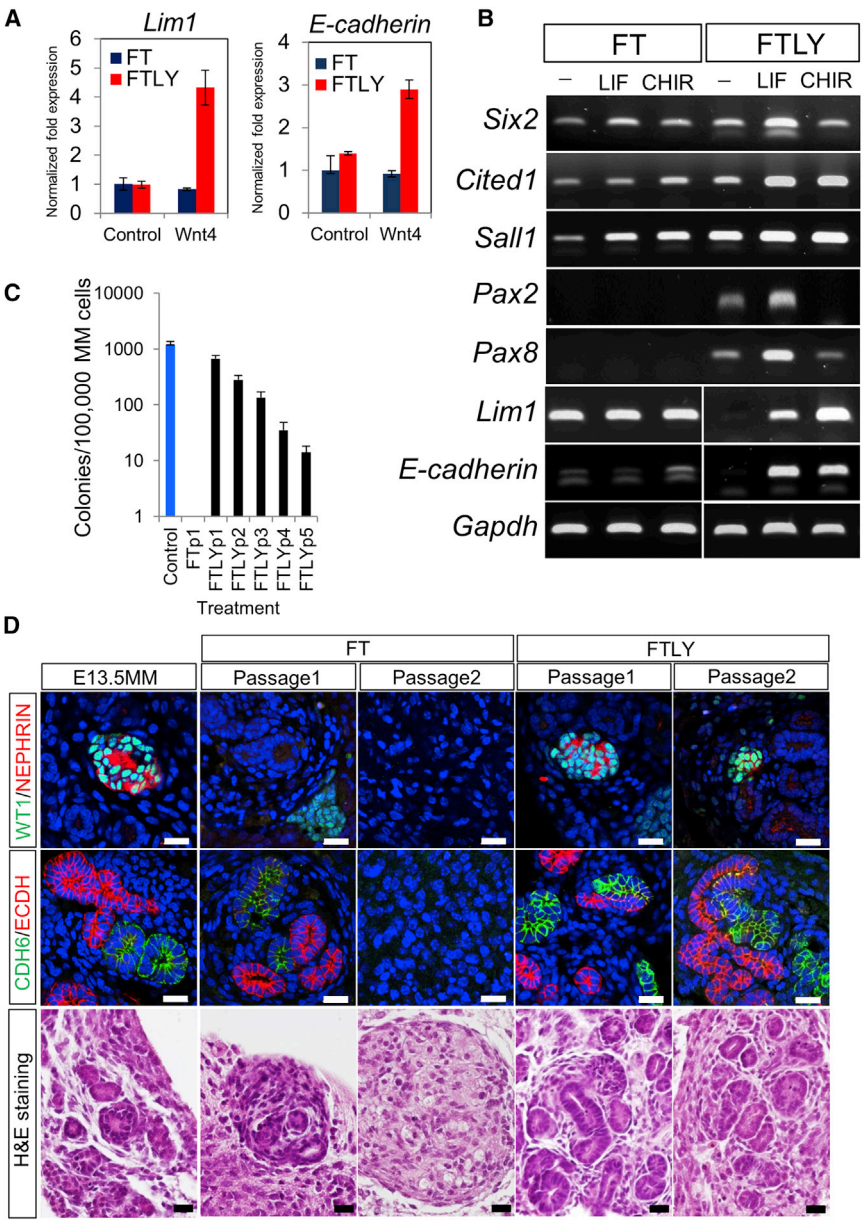

Figure 3. FTLY-Treated rMMs Remain Competent to Respond to Induction and Form Tubules

(A) WNT4 (100 ng/ml) induces the differentiation markers *Lim1* or *E-cadherin* in FTLY-treated rMMs. Cells were treated for 72 hr and analyzed by qPCR.

(B) Passaged FTLY-treated rMM cells also respond to inductive cues. Passage 5 cells treated with LIF (50 ng/ml) or CHIR99021 (CHIR, 1μM) for 72 hr upregulate *Lim1* and *E-cadherin*, as shown by RT-PCR.

(C) Passaged FTLY-treated rMM cells form colonies on NIH 3T3WNT4 feeder cells. Isolated rMM cells served as controls.

(D) rMM cells propagated in FTLY medium form mature renal tubules and glomerular-like structures. rMM cells cultured and passaged in FT or FTLY medium were H&E-stained or probed for expression of the nephronic markers WT1 (condensed mesenchyme or podocytes), NEPHRIN (podocytes/glomeruli), CADHERIN6 (CDH6, proximal tubules), and E-CADHERIN (ECDH, distal tubules). Scale bars, 50 μm.

of a fibronectin-coated, 12-well plate in DMEM with 10% fetal bovine serum (FBS). The following day, 100,000 rMM cells were added per well in a colony assay medium. Only sizable colonies (>10 cells) were counted. In this study, no colonies were observed in co-cultures containing 100,000 rMM cells propagated in FT control medium for 10 days, whereas cells grown in FTLY medium for 10 days sustained the ability to form colonies at a level greater than 50% that of uncultured rMMs (Figure 3C). The frequency of colony formation declined with passage, but small numbers of WNT4-responsive colonies were consistently observed even at passage 5, again demonstrating the preservation of a competent progenitor population in these cultures.

Cultured cells were also assessed for their ability to form nephronic epithelia and undergo segmentation. For this, cells maintained in FT or FTLY medium were passaged and then co-cultured with embryonic spinal cord. Initially, 100,000 rMM cells were allowed to aggregate in wells of a 96-well, low-binding affinity plate for 48 hr and then transferred to filters with embryonic spinal cord. They were then cultured for 8 days on medium with 10% FBS. Under these conditions, control (FT-treated) cells at first passage yielded small, necrotic aggregates with some primitive epithelia that were devoid of any glomerulus-like structures (Figure 3D). Some aggregates expressed WT1, a marker of condensed mesenchyme, and the epithelia exhibited ECDH or CDH6 staining, which label distal and proximal tubules, respectively. However, NEPHRIN, a glomerular marker, was never detected. This is consistent with the induction of primitive epithelia by FGF2 (Karavanov et al., 1998). By passage 2, all FT-treated cultures failed to form even primitive epithelia or stain for any nephron markers (Figure 3D). On the other hand, FTLY-treated and passaged

cells were expanded dramatically, preserved well, and populated with numerous tubules and glomerulus-like structures at both passages (Figure 3D; Figures S4A and S4B). NEPHRIN staining was demonstrable in glomerulus-like foci, and expression of both CDHs was robust. Therefore, FTLY medium preserved the competence of progenitors to form mature segmented nephronic epithelia. Attempts to induce later-passage cells with embryonic spinal cord, however, were unsuccessful. This likely reflects the depletion of SIX2+ progenitors at passage 3, but, as noted, their loss did not preclude the ability of the remaining cells to respond to inductive signals.

Mouse MM Progenitors Are Also Preserved with LIF/ROCKi Treatment

In addition to rat MM cells, comparable culture conditions were applied to mMM cells isolated from E11.5 embryos. Cells were expanded with FTLY medium and then passaged in FT medium with or without LIF or Y27632 for 48 hr. By IF, the majority of cells showed nuclear SIX2 staining in LIF-treated cultures, whereas only a small fraction of cells in FT-treated cultures had stained nuclei (Figure S5A). Furthermore, the expression of stem cell markers after 10 days was preserved only with the addition of LIF (Figure S5B). At 1–5 ng/ml, the expression of *Six2*, *Cited1*, and *Sall1* was robust, and *E-cadherin* was minimized. Furthermore, when FTLY-treated cells were exposed to the GSK3β inhibitor CHIR99021, both *Lim1* and *E-cadherin* were upregulated (Figure S5C), suggesting that mMM also remained competent to respond to induction.

LIF Activates STAT Signaling to Sustain SIX2

LIF functions primarily through the activation of a Janus kinase to phosphorylate a STAT molecule, which then oligomerizes and moves to the nucleus for transcriptional activation (Stephens et al., 1998). Phosphorylation occurs within minutes of LIF exposure. However, STAT upregulates its own expression, yielding high levels of an unphosphorylated form (U-STAT), which also binds DNA (Timofeeva et al., 2012) to activate or repress gene transcription (Yang and Stark, 2008). Multiple STAT family members are expressed in the developing metanephros (Wang et al., 2010), so we assessed the ability of LIF to induce phosphorylation of those STATs. Although 1 ng/ml LIF is optimal for rMM self-renewal, we reported that higher levels (50 ng/ml) induce MET in progenitors (Plisov et al., 2001). Therefore, we evaluated phosphorylation at both concentrations. In rMM cells, STATs 1, 3, 4, 5, and 6 were all expressed and could be activated by LIF. However, LIF stimulated the phosphorylation of only STATs 1, 3, and 5 at 1 ng/ml, suggesting that these STATs mediate LIF signals in our progenitors (Figure 4A). Y27632 elicited no effect on STAT phosphorylation. These

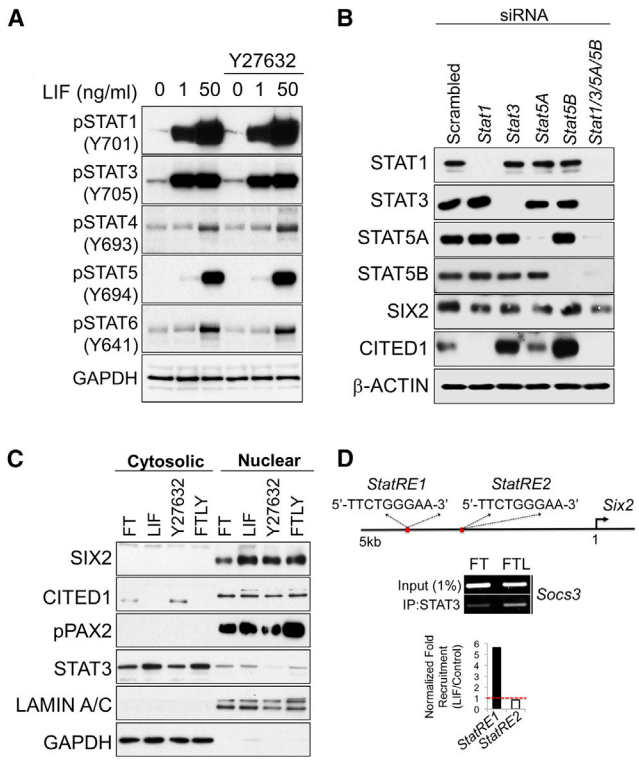

Figure 4. LIF Activates STATs, which Regulate SIX2 Expression

(A) LIF induces phosphorylation of multiple STATs in a dose-dependent manner. Passaged rMM cells were treated with LIF for 15 min.

(B) *Stat* siRNA knockdown inhibits SIX2 expression. rMM cells were analyzed 72 hr after transfection.

(C) LIF and Y27632 enhance nuclear levels of SIX2 and pPAX2. GAPDH marks the cytosolic fraction and LAMIN A/C the nuclear fraction.

(D) STAT3 binds to the *Six2* proximal promoter in primary mMM cells. Top: schematic of two putative *Stat* response elements (*StatRE*) within the 5-kb upstream proximal promoter of the mouse *Six2* locus. Center: ChIP-PCR demonstrating that the promoter-established STAT3 target *Socs3* is bound by STAT3 in response to LIF. Bottom: ChIP qPCR analysis revealing binding of STAT3 to the upstream (*StatRE1*) region of *Six2* under LIF-stimulated conditions. mMM cells were treated until confluency with FT or FTL (LIF = 5 ng/ml) prior to fixation. IP, immunoprecipitation.

findings confirm that LIF activates canonical STAT signaling in cultured rMM cells and establishes redundancy in STAT responses to LIF.

To directly assess the role of STAT signaling in the maintenance of the stem cell phenotype, *Stats* were knocked down individually or collectively with small interfering RNA (siRNA) in rMM cells monitored for SIX2 expression (Figure 4B). Cells (10^6) were transfected using Lipofectamine RNAi MAX and cultured for 3 days in a fibronectin-coated 12-well plate. Consistent with a role in stem cell

stabilization, knockdown (KD) of *Stats 1*, *3*, or *5* individually showed reduced levels of SIX2 expression. Furthermore, the greatest SIX2 reduction was observed with KD of all three *Stats*. The resulting partial attenuation of SIX2 may either reflect the involvement of other factors in regulating its expression or possibly the loss of preferential growth of the SIX2+ progenitor. Nuclear levels of stem cell markers were also evaluated in cells treated with FT plus LIF (1 ng/ml) or Y27632 after 3 days in culture. Individually, both LIF and Y27632 treatments increased nuclear SIX2 levels (Figure 4C). Furthermore, the combination greatly increased nuclear levels of pPAX2. FGF2 is known to activate STAT signaling (Megeney et al., 1996), so it is not surprising that FT (control) medium also induced nuclear STAT3. LIF, however, overcame the attenuating effects of Y27632 on nuclear STAT3. These studies suggest that both LIF and Y27632 regulate nuclear levels of SIX2 and PAX2, but, again, this result could be explained either by growth selection of the SIX2+ cell or by induction of expression.

Because cytosolic SIX2 was not demonstrable in immunoblots (Figure 4C), we hypothesized that this transcription factor is unstable outside of the nucleus. To test this, cells were exposed to the proteasomal inhibitor MG132 and harvested as above. Under these conditions, a prominent cytosolic band of the appropriate size was detected (Figure S6A), indicating that SIX2 is degraded rapidly in the cytoplasm and suggesting that any cytoplasmic IF staining for SIX2 is attributable to its degradation products.

To better understand a possible relationship between STAT activation and *Six2* expression, we examined direct binding of STAT3 to the *Six2* promoter using a chromatin immunoprecipitation (ChIP) assay. Because the mouse genome has been much more rigorously sequenced and annotated in the *Six2* promoter than the rat genome, mMM cells were used for ChIP analysis. Isolated mMM cells were propagated in FT or FTL (5 ng/ml LIF) medium to confluence (6–8 days). In silico analysis of the *Six2* proximal promoter revealed two clearly defined *Stat* consensus binding sites (*StatRE1* and *StatRE2*) within 5 kb of the start codon (Figure 4D, top). *Socs3* is a well established direct target for STAT3 binding and was included as a positive control (Figure 4D, center). LIF treatment significantly increased STAT3 binding to the *Socs3* promoter, demonstrating the efficacy of the procedure. Similarly, STAT3 binding to the *Six2* promoter was enhanced with LIF treatment, exhibiting a nearly 6-fold enrichment in recruitment to the *Six2 StatRE1* relative to *StatRE2* (Figure 4D, bottom). Therefore, STAT3 binds directly to the *Six2* promoter. Given that binding is plotted relative to an internal control, a lower-affinity *StatRE2* site, the 6-fold differential between StatRE1 and StatRE2 is likely due to a bona fide increase in binding rather than merely a selection for the SIX2+ progenitor, although we cannot rule out the latter.

LIF Differentially Activates PLCγ to Suppress SIX2 Expression

As mentioned above, LIF mediates opposing concentration-dependent activities in rMM cells. To better understand the basis for this, we evaluated the ability of LIF to activate CALCINEURIN/calcium signaling as described previously for Wnt4 (Tanigawa et al., 2011). When cultured rMMs were induced with 50 ng/ml LIF, both differentiation markers, *Lim1* and *E-cadherin*, were upregulated after 6 days of treatment (Figure 5A). However, cyclosporine A (CsA), a CALCINEURIN/NFAT inhibitor, blocked the ability of LIF to induce the expression of these markers, whereas the β-CATENIN inhibitor CT-HC-1 had no effect on differentiation. Therefore, both LIF and WNT4 mediate MET through a calcium-dependent mechanism. Because the PHOSPHOLIPASE C (PLC) metabolite inositol 1,4,5-trisphosphate stimulates calcium release and uptake and because JAK/STAT signaling can also initiate a calcium cascade through PLC activation (Soriano et al., 2003), we evaluated PLC phosphorylation following treatment of rMMs with 1 or 50 ng/ml LIF. As shown in Figure 5B, 1 ng/ml LIF induced a small, brief elevation of PLCγ1 phosphorylation for a 5- to 10-min time period, whereas 50 ng/ml LIF caused a robust increase in phosphorylation for at least 60 min. Simultaneously, pSTAT3 and 5 remained greatly elevated at both LIF concentrations, suggesting that a differential in PLCγ1 phosphorylation may contribute to the concentration-dependent responses and that this balance may help determine when the progenitor commits or self-renews. Conversely, knockdown of PLCγ1 over 72 hr caused an increase in SIX2 levels in immunoblots of FTLY-cultured rMMs (Figure 5C), suggesting that it may play a regulatory role in lineage commitment.

Y27632 Attenuates JNK Signaling and Activates *Slug* Expression when Combined with LIF

JNK inhibitors block expression of differentiation markers, including *E-cadherin*, in mMMs (Osafune et al., 2006). In rMM cells, 1 ng/ml LIF weakly activated the 46-kDa form of pJNK, whereas 50 ng/ml greatly elevated phosphorylation of both the 46- and 55-kDa pJNK isoforms after only 15 min of treatment (Figure 5D). Moreover, the JNK inhibitor SP600125 abrogated the expression of *Lim1* and *E-cadherin* in rMM cells treated for 6 days (Figure 5E). The EMT regulatory factor *Slug/Snai2*, which is expressed in MM progenitors (Savagner et al., 1998), was also evaluated in response to LIF treatment. LIF (50 ng/ml) inhibited *Slug* expression in rMMs treated for 6 days (Figures 5F and 5G) unless partnered with a JNK inhibitor with which it stimulated *Slug* levels instead (Figure 5G). These findings provide strong evidence that LIF plays a dual role in cells. Through STAT signaling, it supports stemness by selecting

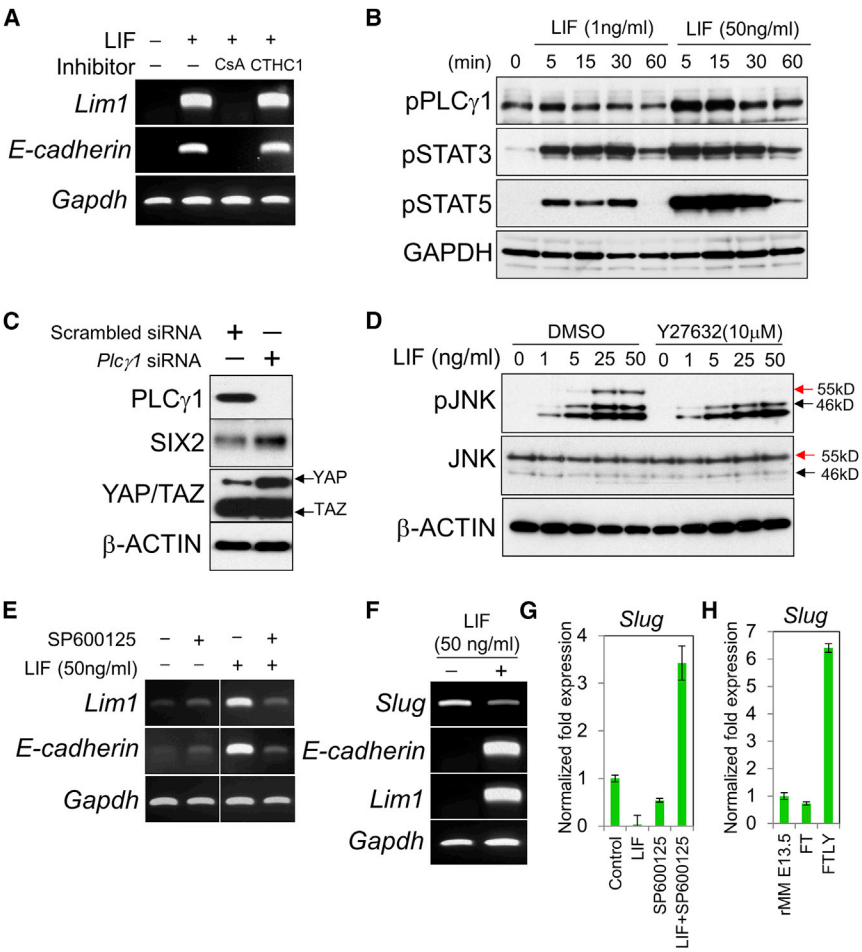

Figure 5. LIF Activates PLCγ and JNK in a Dose-Dependent Manner

(A) Calcium/NFAT signaling mediates LIF-induced MET. rMMs were treated with LIF (50 ng/ml) in the presence of the calcium/NFAT inhibitor CsA (10 μM) or the β-CATENIN inhibitor CT-HC-1 (10 μM) for 6 days and analyzed for the MET markers *Lim1* and *E-cadherin*.

(B) LIF differentially activates PLCγ. Passaged rMM cells were treated with 1 or 50 ng/ml LIF.

(C) PLCγ negatively regulates SIX2 and YAP expression. rMM cells transfected with *Plcγ* siRNA were harvested after 72 hr.

(D) Y27632 attenuates LIF-induced JNK phosphorylation. Cells were pretreated with Y27632 (10 μM) for 30 min and then with LIF for 15 min.

(E) JNK facilitates LIF-induced MET in rMMs. rMMs were treated with LIF (50 ng/ml) or the JNK inhibitor SP600125 (10μM) for 6 days.

(F) LIF suppressed *Slug/Snai2* expression during MET. rMMs were treated with LIF (50 ng/ml) for 6 days.

(G) SP600125 reverses the LIF-induced suppression of *Slug* in rMM cells. rMMs were treated with LIF (50 ng/ml) or SP600125 (10μM) for 6 days.

(H) LIF (1 ng/ml) plus Y27632 stimulates *Slug* expression in cultured rMM cells.

SIX2+ cells or inducing SIX2 expression while also activating PLC and JNK to facilitate MET.

Rho kinase regulates JNK signaling by activating/phosphorylating JNK itself (Marinissen et al., 2004). As predicted, Y27632 attenuates JNK phosphorylation of both the 46- and 55-kD isoforms (Figure 5D). Interestingly, LIF with Y27632 also stimulated *Slug* expression in rMMs treated for 6 days (Figure 5H), as observed with the JNK inhibitor (Figure 5G). These findings suggest that Y27632 helps maintain rMMs by inhibiting their differentiation through attenuation of JNK activity.

LIF Induces YAP, which Regulates Several rMM Stemness Markers

YAP is involved in the regulation of MM progenitors both in vivo and in short-term primary culture (Das et al., 2013). In those studies, it was predominantly nuclear localized in cultured cells at low density but lost from nuclei in rMM cells cultured for 72 hr at high density (arrows), as shown in Figure 6A. In contrast, FTLY-treated rMM progenitors showed nuclear YAP in cells regardless of density, suggesting that FTLY overcomes any density-dependent repression of YAP signaling. To further investigate this phenomenon, rMM progenitors were cultured in FT medium with LIF or Y27632 for 72 hr and evaluated for YAP or TAZ (Figure 6B). Although cytosolic levels of YAP/TAZ were similar regardless of treatment, 1 ng/ml LIF greatly increased the nuclear levels of both. Interestingly, Y27632 abrogated this response, but the effect could then be rescued with LIF. These studies suggest that LIF may activate YAP signaling in rMM cells and demonstrate that LIF and Y27632 play distinct but complementary roles in maintaining the MM progenitor.

To determine whether YAP also stabilizes stem marker expression in rMM progenitors, FTLY-treated cells were transfected with *Yap* siRNA and cultured for 72 hr. This resulted in a substantial loss of YAP and the downregulation of expression of all stem markers, including SIX2, CITED1, PAX2, and SALL1 (Figure 6C), suggesting that it plays a major role in the regulation of key stem cell regulatory factors. *Yap* knockdown also caused a concomitant increase in the expression of the differentiation markers *Pax8*, *E-cadherin*,

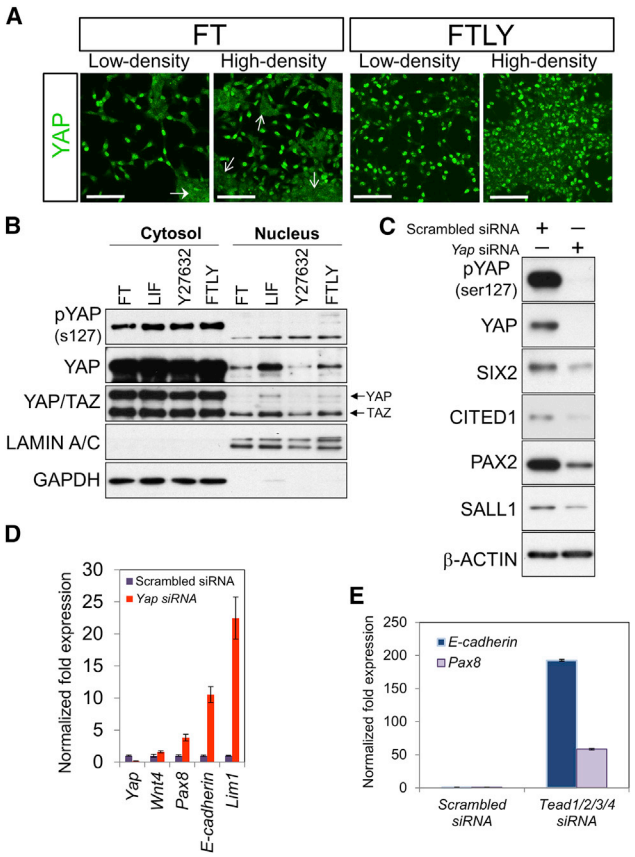

Figure 6. YAP Regulates Progenitor Markers

(A) LIF and Y27632 override density-dependent signals for nuclear localization of YAP. White arrows indicate dense areas lacking Yap nuclear localization. Scale bars, 100 μm.

(B) LIF increases nuclear levels of YAP/TAZ. Cells were cultured for 72 hr (LIF, 1 ng/ml). GAPDH and LAMIN A/C distinguished fractions.

(C) *Yap* knockdown decreased progenitor marker expression in rMM cells.

(D) Silencing *Yap* increased the expression of differentiation markers in rMM cells.

(E) *Tead* knockdown upregulated differentiation markers in rMM cells.

and *Lim1* (Figure 6D). Conversely, knockdown of PLCγ not only upregulated SIX2 expression, as described earlier, but also upregulated YAP expression (Figure 5C). This suggests that YAP and calcium signaling function in tandem to balance MM progenitor commitment to nephronic differentiation and that loss of nuclear YAP is sufficient to permit MET.

YAP Functions in MM Progenitors by a TEAD-Dependent Mechanism

To directly determine whether the canonical YAP transcriptional partner TEAD mediates YAP activity in rMMs, all four TEAD family members were knocked down collectively in cells, which were then analyzed for the induction of the differentiation markers *E-cadherin* and *Pax8*. Expression levels for each individual TEAD were depressed significantly following knockdown (Figure S6B) and resulted in an upregulation of both *Pax8* and *E-cadherin* (Figure 6E). Therefore, YAP likely functions through TEAD activation to suppress the differentiation of rMM progenitors.

DISCUSSION

In this study, we define serum-free culture conditions that permit the massive, rapid, and preferential expansion of SIX2+ MM progenitors with the preservation of a stem-like phenotype. Furthermore, the cells derived from these conditions retain their capacity to form nephronic tubules and glomeruli when induced with embryonic spinal cord and remain responsive to inductive signals after multiple passages. This is the first evidence showing that functional nephronic progenitors can be maintained in culture long-term. We also demonstrate the efficacy of genetically manipulating these cells and interrogating specific signaling mechanisms through gene-targeted knockdowns.

Previously we reported the propagation of rMM progenitors with FT medium and short-term retention of functionality (Tanigawa et al., 2011), but, here, we demonstrate that cells lose *Six2* and *Pax2* expression in primary culture and become unresponsive to inductive signals. SIX2+/PAX2− mMMs were passaged successfully as nephrospheres, but the cells failed to epithelialize at any passage (Lusis et al., 2010). PAX2 facilitates competency in mMM progenitors, allowing them to undergo MET (Brophy et al., 2001), and is likely required for the long-term inducibility of these cells. As shown here, the combination of LIF and Y27632 sustained *Pax2* expression in rMMs and stimulated nuclear levels of pPAX2. Therefore, both SIX2 and PAX2 may be functional determinants for the successful culture of nephronic stem cells.

FTLY preferentially expanded the SIX2+ population in our mixed MM cultures. The exact basis for this is unknown but may be due to the elaboration of the LIF receptor on cap mesenchyme cells (Plisov et al., 2001). In embryonic rat kidney, LIFR antibody labeled the membranes of cap cells, whereas membrane staining of the interstitial stroma was not apparent. By whatever mechanism, the selectivity complicates our findings because many of our experiments were performed over a 7- to 10-day period, during which selection had occurred. Regardless, the use of an internal low-affinity binding site as the control should have partially mitigated any selectivity in our ChIP experiments. Moreover, the combination of STAT redundancy, partial

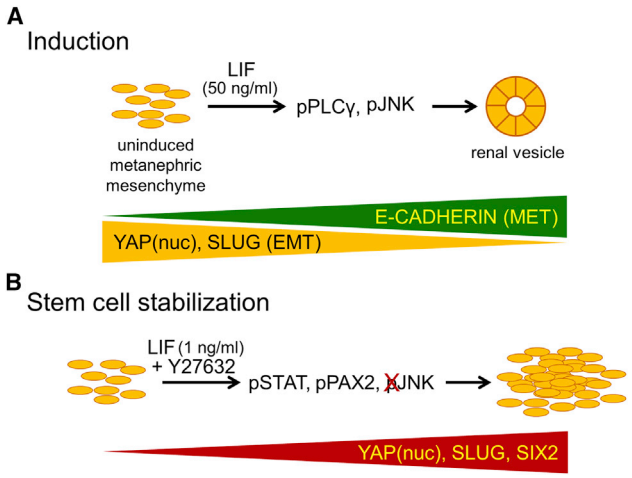

Figure 7. Model of MM Induction (A) or Stem Cell Stabilization (B) Based on Our Findings with LIF and Y27632.

retention of SIX2, and 3-day time points should have precluded the selective loss of SIX2+ cells in the *Stat* knockdown studies. Still, further study of the direct role of LIF on *Six2* expression in these cells is clearly warranted.

We demonstrate that LIF affects signaling in MM progenitors in a concentration-dependent manner (Figure 7; Figure S7). At 1 ng/ml, it induces phosphorylation primarily of STATs 1, 3, and 5 as well as the expression of several progenitor markers, whereas, at 50 ng/ml, it additionally activates both PLCγ and JNK. Because the higher concentration of LIF is associated with the induction of MET and nephronic tubule formation (Barasch et al., 1999; Plisov et al., 2001), it is possible that PLCγ and JNK are involved in those morphogenetic processes. The PLCγ metabolite IP3 activates PROTEIN KINASE C, which initiates an intracellular calcium cascade. Because knockdown of PLCγ upregulated the expression of the stem markers SIX2 and YAP, it is likely that LIF-activated PLCγ helps override the stemness program to direct cells to form tubules. This is supported by the fact that *PLCγ*-deficient chimeric mice develop cystic kidneys, a symptom of aberrant tubular proliferation (Shirane et al., 2001).

In this study, LIF also induced JNK phosphorylation and upregulated the expression of the differentiation markers *Lim1* and *E-cadherin*. This induction was attenuated by treatment with a JNK inhibitor. Furthermore, both the JNK and ROCK inhibitors facilitated expression of the progenitor marker *Slug* but, interestingly, only in concert with LIF. These findings suggest that the role of Y27632 may be to limit the LIF-induced, JNK-mediated differentiation of rMMs and, instead, help sustain cells in a more primitive state.

Yap plays a major role in maintaining the pluripotency of mouse ESCs (mESCs), and LIF is in part responsible for sustaining YAP expression in those cells (Tamm et al., 2011). In turn, YAP stimulates LIF receptor expression, facilitating mESC competency to respond to LIF. Furthermore, YAP complexes with a TEAD family member to activate transcription of LIF-dependent targets in mESCs. We provide the first evidence showing that LIF functions similarly in MMs by increasing nuclear levels of YAP and sustaining the expression of several MM stemness markers. We also found that YAP signals in MMs through a canonical mechanism involving TEAD transcriptional activation, as observed for mESCs. *Tead-2/4* are both expressed in MMs (GUDMAP, Andrew P. McMahon lab) and are therefore the most likely to co-localize with YAP/TAZ (Das et al., 2013). Moreover, FTLY stimulated proliferation of MM progenitors and permitted nuclear localization of YAP even in areas of high density. This suggests that the combined treatment of LIF and Y27632 on MM cells constitutively activates YAP and may explain not only the dramatic growth observed in treated cultures but also the retention of a stem-like phenotype of the progenitors in long-term cultures.

Although our studies bring new attention to the role of LIF/JAK/STAT signaling in regulating stemness of the MM progenitor, we have yet to address how this may interface with the established role of β-CATENIN in this process. Mouse genetic studies have clearly implicated canonical WNT signaling in the maintenance of the MM progenitor (Karner et al., 2011; Park et al., 2007). Because a combination of LIF and a WNT is sufficient to support the expansion of germline-competent mouse ESCs (ten Berge et al., 2011), it is intriguing that both may also be necessary for the long-term propagation of MM progenitors. As indicated, our current conditions do not preserve the capacity of cells to form tubules over several passages. This is likely due to the depletion of progenitors that commit spontaneously to primitive epithelia. Perhaps a deficiency in canonical WNT signaling is responsible, a possibility currently under investigation.

EXPERIMENTAL PROCEDURES

Tissues and Primary MM Cell Cultures

Metanephric mesenchymes were enzymatically separated from T-shaped ureteric buds of E13.5 rat or E11.5 mouse embryos as described previously (Perantoni et al., 1991) and cultured as described by Tanigawa et al. (2011). Cells were dissociated with 0.25% trypsin-EDTA solution (Gibco-Invitrogen) and washed with PBS for passaging.

Cell Proliferation Assay

Primary cultures of rMM cells were trypsinized, and cells (1–9 × 10^4 cells/well) were plated in a 96-well plate and treated as indicated for 72 hr. Cell viability and growth were assessed using

WST-1 cell proliferation reagent (Roche Applied Science) according to manufacturer's instructions.

Population Analysis

Cells were seeded in four-chamber fibronectin-coated slides at 50,000 cells/chamber, fixed after 24 hr (unless expanded as primaries for 7 days), and probed for SIX2 (nephronic progenitors) or PBX1 (stroma). Counts of cells with stained nuclei were compiled from an analysis of 500–2,000 cells/slide using a Zeiss LSM710 confocal microscope. All points were generated from three independent cultures.

Colony Assay

Colony formation by MM progenitors was performed as described previously (Osafune et al., 2006) with minor modifications. A clone of WNT4-expressing NIH 3T3 cells (Andreas Kispert) was selected for high WNT4 expression (Jeffrey Rubin) and used as a feeder layer for these studies. Mitomycin C-treated feeder cells were seeded in 12-well dishes (500,000 cells/well) in DMEM with 10% FBS. The following day, the medium was replaced with colony assay medium, and MM cells (100,000/well) were added. Colony formation was assessed after 7 days.

Animals

All animal procedures were performed following guidelines from the National Cancer Institute (NCI)-Frederick Animal Care and Use Committee. NCI-Frederick is accredited by the Association for Assessment and Accreditation of Laboratory Animal Care International and follows the Public Health Service Policy for the Care and Use of Laboratory Animals. Animal care was provided in accordance with the procedures outlined in the Guide for Care and Use of Laboratory Animals (National Research Council, 1996, National Academy Press, Washington, D.C.).

Semiquantitative RT-PCR

Analyses were performed as described previously (Tanigawa et al., 2011). Primer sequences, annealing temperatures, and cycle parameters are shown in Table S1.

Immunoblotting

Immunoblotting was performed as described previously (Tanigawa et al., 2011).

Cell Fractionation

Nuclear and cytosolic proteins were prepared according to Dignam et al. (1983). Briefly, cells were treated for 72 hr, harvested in cold PBS, and pelleted (500 × *g*) for 5 min. Pellets were lysed with buffer A (10 mM HEPES-KOH [pH 7.9], 10 mM KCl, 0.1 mM EDTA, 0.5% Nonidet P-40, 1 mM dithiothreitol, and 0.5 mM phenylmethylsulfonyl fluoride [PMSF]) on ice for 20 min and centrifuged (14,000 × *g*) for 15 min at 4°C. Supernatants served as cytoplasmic fractions. Nuclear pellets were washed three times with buffer A and resuspended in buffer B (20 mM HEPES, 0.5 M KCl, 1 mM EDTA, 1 mM dithiothreitol, and 1 mM PMSF [pH 7.9]) for 30 min at 4°C on a rotating wheel and centrifuged at 14,000 × *g* for 15 min at 4°C. One part of the cytosolic and nuclear fractions was analyzed using anti-LAMIN A/C or anti-GAPDH antibody. Protein concentration was determined using a protein assay kit (Bio-Rad) according to the manufacturer's instructions.

Plasmids and Electroporation

Transfections were performed as described previously (Tanigawa et al., 2011), except with 2 μg plasmid and 5×10^5 cells/transfection. After 24 hr, cells were harvested with TRIzol reagent (Invitrogen) for RNA isolation. Transfection efficiencies were greater than 90%.

siRNA Transfection

siRNA reagents were transfected into rat MM cells by Lipofectamine RNAi MAX (Invitrogen) reagent using the manufacturer's protocol. The culture medium was changed 24 hr after transfection, and transfection efficiency was analyzed by qRT-PCR or immunoblotting.

Immunocytochemistry/Immunofluorescence

Primary MM cells were cultured on four chamber matrix-coated slides. Cells were fixed (4% paraformaldehyde/10 min) and processed according to Abcam's immunocytochemistry protocol (http://www.abcam.com/index.html?pageconfig=popular_protocols), blocking with 10% goat serum and mounting in Vectashield (Vector Laboratories). Cells were visualized on an LSM710 confocal microscope (Carl Zeiss) and analyzed by ZEN image software (Zeiss). IF staining for nephron segment-specific markers was performed as described previously (Taguchi et al., 2014).

Chromatin Immunoprecipitation Assay

The 5-kb upstream promoter region of mouse *Six2* was interrogated for known transcription factor binding elements using the web-based TFSearch program (http://diyhpl.us/~bryan/irc/protocol-online/protocol-cache/TFSEARCH.html). "*Statx*" sites with a score of ≥90 were probed for STAT3 binding by ChIP. Primary mMM cells were cultured as described previously in FT medium with or without LIF (5 ng/ml) for 6–8 days in 60-mm dishes. ChIP was done as described previously (Lee et al., 2006). Briefly, cells were fixed (1% paraformaldehyde/15 min) and sonicated (60 min) on ice using a Bioruptor at low power and a 30-s on/off oscillation program (average fragmentation of 500–1,000 bp). Recruitment of STAT3 to target DNA elements was evaluated by PCR or qPCR following immunoprecipitation of STAT3 (Cell Signaling Technology, antibody 9139S). Primers are shown in Table S1.

Statistical Analysis

Data were evaluated as described previously using Student's t test (Tanigawa et al., 2011). All experiments were performed independently at least three times. Error bars represent the variation from three or more independent experiments.

SUPPLEMENTAL INFORMATION

Supplemental Information includes Supplemental Experimental Procedures, seven figures, and one table and can be found with this article online at http://dx.doi.org/10.1016/j.stemcr.2015.07.015.

ACKNOWLEDGMENTS

This work was supported by a fellowship from the Japanese Society for the Promotion of Science (to S.T.), grant KAKENHI 26860640 from the Ministry of Education, Culture, Sports, Science and Technology (MEXT) of Japan (to S.T.), and the Intramural Research Program of the NIH, NCI, CCR. We thank Drs. Taguchi, Kaku, Ohmori, and Fujimura for technical guidance. We thank Drs. Lewandoski and Mackem for a critical review of the manuscript.

Received: January 12, 2015
Revised: July 30, 2015
Accepted: July 31, 2015
Published: August 27, 2015

REFERENCES

Barak, H., Huh, S.H., Chen, S., Jeanpierre, C., Martinovic, J., Parisot, M., Bole-Feysot, C., Nitschké, P., Salomon, R., Antignac, C., et al. (2012). FGF9 and FGF20 maintain the stemness of nephron progenitors in mice and man. Dev. Cell *22*, 1191–1207.

Barasch, J., Yang, J., Ware, C.B., Taga, T., Yoshida, K., Erdjument-Bromage, H., Tempst, P., Parravicini, E., Malach, S., Aranoff, T., and Oliver, J.A. (1999). Mesenchymal to epithelial conversion in rat metanephros is induced by LIF. Cell *99*, 377–386.

Blank, U., Brown, A., Adams, D.C., Karolak, M.J., and Oxburgh, L. (2009). BMP7 promotes proliferation of nephron progenitor cells via a JNK-dependent mechanism. Development *136*, 3557–3566.

Boivin, F.J., Sarin, S., Lim, J., Javidan, A., Svajger, B., Khalili, H., and Bridgewater, D. (2015). Stromally expressed β-catenin modulates Wnt9b signaling in the ureteric epithelium. PLoS ONE *10*, e0120347.

Brophy, P.D., Ostrom, L., Lang, K.M., and Dressler, G.R. (2001). Regulation of ureteric bud outgrowth by Pax2-dependent activation of the glial derived neurotrophic factor gene. Development *128*, 4747–4756.

Buehr, M., Meek, S., Blair, K., Yang, J., Ure, J., Silva, J., McLay, R., Hall, J., Ying, Q.L., and Smith, A. (2008). Capture of authentic embryonic stem cells from rat blastocysts. Cell *135*, 1287–1298.

Cho, E.A., Patterson, L.T., Brookhiser, W.T., Mah, S., Kintner, C., and Dressler, G.R. (1998). Differential expression and function of cadherin-6 during renal epithelium development. Development *125*, 803–812.

Das, A., Tanigawa, S., Karner, C.M., Xin, M., Lum, L., Chen, C., Olson, E.N., Perantoni, A.O., and Carroll, T.J. (2013). Stromal-epithelial crosstalk regulates kidney progenitor cell differentiation. Nat. Cell Biol. *15*, 1035–1044.

Dignam, J.D., Lebovitz, R.M., and Roeder, R.G. (1983). Accurate transcription initiation by RNA polymerase II in a soluble extract from isolated mammalian nuclei. Nucleic Acids Res. *11*, 1475–1489.

Ekblom, P., Alitalo, K., Vaheri, A., Timpl, R., and Saxén, L. (1980). Induction of a basement membrane glycoprotein in embryonic kidney: possible role of laminin in morphogenesis. Proc. Natl. Acad. Sci. USA *77*, 485–489.

Karavanov, A.A., Karavanova, I., Perantoni, A., and Dawid, I.B. (1998). Expression pattern of the rat Lim-1 homeobox gene suggests a dual role during kidney development. Int. J. Dev. Biol. *42*, 61–66.

Karner, C.M., Das, A., Ma, Z., Self, M., Chen, C., Lum, L., Oliver, G., and Carroll, T.J. (2011). Canonical Wnt9b signaling balances progenitor cell expansion and differentiation during kidney development. Development *138*, 1247–1257.

Kobayashi, A., Valerius, M.T., Mugford, J.W., Carroll, T.J., Self, M., Oliver, G., and McMahon, A.P. (2008). Six2 defines and regulates a multipotent self-renewing nephron progenitor population throughout mammalian kidney development. Cell Stem Cell *3*, 169–181.

Lee, T.I., Johnstone, S.E., and Young, R.A. (2006). Chromatin immunoprecipitation and microarray-based analysis of protein location. Nat. Protoc. *1*, 729–748.

Lusis, M., Li, J., Ineson, J., Christensen, M.E., Rice, A., and Little, M.H. (2010). Isolation of clonogenic, long-term self renewing embryonic renal stem cells. Stem Cell Res. (Amst.) *5*, 23–39.

Marinissen, M.J., Chiariello, M., Tanos, T., Bernard, O., Narumiya, S., and Gutkind, J.S. (2004). The small GTP-binding protein RhoA regulates c-jun by a ROCK-JNK signaling axis. Mol. Cell *14*, 29–41.

Megeney, L.A., Perry, R.L., LeCouter, J.E., and Rudnicki, M.A. (1996). bFGF and LIF signaling activates STAT3 in proliferating myoblasts. Dev. Genet. *19*, 139–145.

Osafune, K., Takasato, M., Kispert, A., Asashima, M., and Nishinakamura, R. (2006). Identification of multipotent progenitors in the embryonic mouse kidney by a novel colony-forming assay. Development *133*, 151–161.

Park, J.S., Valerius, M.T., and McMahon, A.P. (2007). Wnt/beta-catenin signaling regulates nephron induction during mouse kidney development. Development *134*, 2533–2539.

Perantoni, A.O., Dove, L.F., and Williams, C.L. (1991). Induction of tubules in rat metanephrogenic mesenchyme in the absence of an inductive tissue. Differentiation *48*, 25–31.

Perantoni, A.O., Dove, L.F., and Karavanova, I. (1995). Basic fibroblast growth factor can mediate the early inductive events in renal development. Proc. Natl. Acad. Sci. USA *92*, 4696–4700.

Perantoni, A.O., Timofeeva, O., Naillat, F., Richman, C., Pajni-Underwood, S., Wilson, C., Vainio, S., Dove, L.F., and Lewandoski, M. (2005). Inactivation of FGF8 in early mesoderm reveals an essential role in kidney development. Development *132*, 3859–3871.

Plisov, S.Y., Yoshino, K., Dove, L.F., Higinbotham, K.G., Rubin, J.S., and Perantoni, A.O. (2001). TGF beta 2, LIF and FGF2 cooperate to induce nephrogenesis. Development *128*, 1045–1057.

Plisov, S., Tsang, M., Shi, G., Boyle, S., Yoshino, K., Dunwoodie, S.L., Dawid, I.B., Shioda, T., Perantoni, A.O., and de Caestecker, M.P. (2005). Cited1 is a bifunctional transcriptional cofactor that regulates early nephronic patterning. J. Am. Soc. Nephrol. *16*, 1632–1644.

Rogers, S.A., Ryan, G., and Hammerman, M.R. (1992). Metanephric transforming growth factor-alpha is required for renal organogenesis in vitro. Am. J. Physiol. *262*, F533–F539.

Savagner, P., Karavanova, I., Perantoni, A., Thiery, J.P., and Yamada, K.M. (1998). Slug mRNA is expressed by specific mesodermal derivatives during rodent organogenesis. Dev. Dyn. *213*, 182–187.

Shirane, M., Sawa, H., Kobayashi, Y., Nakano, T., Kitajima, K., Shinkai, Y., Nagashima, K., and Negishi, I. (2001). Deficiency of phospholipase C-gamma1 impairs renal development and hematopoiesis. Development *128*, 5173–5180.

Soriano, S.F., Serrano, A., Hernanz-Falcón, P., Martín de Ana, A., Monterrubio, M., Martínez, C., Rodríguez-Frade, J.M., and Mellado, M. (2003). Chemokines integrate JAK/STAT and G-protein pathways during chemotaxis and calcium flux responses. Eur. J. Immunol. *33*, 1328–1333.

Stephens, J.M., Lumpkin, S.J., and Fishman, J.B. (1998). Activation of signal transducers and activators of transcription 1 and 3 by leukemia inhibitory factor, oncostatin-M, and interferon-gamma in adipocytes. J. Biol. Chem. *273*, 31408–31416.

Taguchi, A., Kaku, Y., Ohmori, T., Sharmin, S., Ogawa, M., Sasaki, H., and Nishinakamura, R. (2014). Redefining the in vivo origin of metanephric nephron progenitors enables generation of complex kidney structures from pluripotent stem cells. Cell Stem Cell *14*, 53–67.

Tamm, C., Böwer, N., and Annerén, C. (2011). Regulation of mouse embryonic stem cell self-renewal by a Yes-YAP-TEAD2 signaling pathway downstream of LIF. J. Cell Sci. *124*, 1136–1144.

Tanigawa, S., Wang, H., Yang, Y., Sharma, N., Tarasova, N., Ajima, R., Yamaguchi, T.P., Rodriguez, L.G., and Perantoni, A.O. (2011). Wnt4 induces nephronic tubules in metanephric mesenchyme by a non-canonical mechanism. Dev. Biol. *352*, 58–69.

ten Berge, D., Kurek, D., Blauwkamp, T., Koole, W., Maas, A., Eroglu, E., Siu, R.K., and Nusse, R. (2011). Embryonic stem cells require Wnt proteins to prevent differentiation to epiblast stem cells. Nat. Cell Biol. *13*, 1070–1075.

Timofeeva, O.A., Chasovskikh, S., Lonskaya, I., Tarasova, N.I., Khavrutskii, L., Tarasov, S.G., Zhang, X., Korostyshevskiy, V.R., Cheema, A., Zhang, L., et al. (2012). Mechanisms of unphosphorylated STAT3 transcription factor binding to DNA. J. Biol. Chem. *287*, 14192–14200.

Torres, M., Gómez-Pardo, E., Dressler, G.R., and Gruss, P. (1995). Pax-2 controls multiple steps of urogenital development. Development *121*, 4057–4065.

Wang, H., Yang, Y., Sharma, N., Tarasova, N.I., Timofeeva, O.A., Winkler-Pickett, R.T., Tanigawa, S., and Perantoni, A.O. (2010). STAT1 activation regulates proliferation and differentiation of renal progenitors. Cell. Signal. *22*, 1717–1726.

Yang, J., and Stark, G.R. (2008). Roles of unphosphorylated STATs in signaling. Cell Res. *18*, 443–451.